



UNIVERSITÀ  
DI PAVIA

Dipartimento di Scienze della Terra e dell'Ambiente

Direttore: Prof. A. Di Giulio

Corso di Laurea in Scienze Geologiche

**GEOthermometric Application on the Graphite of  
Yamato 74123 Ureilite**

Relatore:

Prof. Maria Chiara Domeneghetti

Correlatrice:

Dr.ssa Anna Barbaro

Tesi di Laurea

in Scienze Geologiche

di LEONARDO RAVIZZA

matr. 454180

Anno Accademico 2019/2020

Dichiaro che la presente tesi sperimentale di  
Laurea Triennale in Scienze Geologiche  
è stata svolta sotto la mia guida e su  
tema da me assegnato, presso il  
Dipartimento di Scienze della Terra e dell'Ambiente  
dell'Università degli Studi di Pavia.

Prof. Maria Chiara Domeneghetti

A handwritten signature in black ink, reading "M. Chiara Domeneghetti". The signature is written in a cursive style with a small flourish at the end.

# TABLE OF CONTENTS

ABSTRACT	4
1 INTRODUCTION	5
1.1 Ureilites	5
1.2 Yamato meteorites	8
2 SAMPLE	10
2.1 Sample description by optical microscopy and scanning electron microscopy (SEM)	10
3 EXPERIMENTAL METHODS	15
3.1 Micro-Raman Spectroscopy (MRS) analyses	15
4 DISCUSSION	18
5 CONCLUSIONS	19
6 REFERENCES	
ACKNOWLEDGEMENTS	24

## ABSTRACT

The aim of this bachelor thesis is the study of graphite in Yamato 74123 sample. I obtained geothermometric data by micro-Raman spectroscopy of non-polished graphite in Y-74123 ureilite from the collection of the Natural History Museum Vienna. In this sample, graphite shows a G-band peak center between 1579 and 1582  $\text{cm}^{-1}$  and a full width at half maximum (FWHM) between 11 and 16  $\text{cm}^{-1}$  corresponding to a crystallization temperature of graphite with values ranging between 1265 and 1334 ( $\pm 120$ )  $^{\circ}\text{C}$ . This temperature range is slightly higher than the previously estimated crystallization temperatures reported for graphite in some Almahata Sitta (AhS) ureilites.

Recent works by X-ray diffraction on Y-74123 and on NWA 7983 ureilites showed that the graphite is associated with abundant nano and micro diamond and argued that this assemblage formed in an impact event. I investigated by micro-Raman Spectroscopy the same Y-74123 sample and propose that the temperature obtained on the graphite on this sample [1100-1300  $^{\circ}\text{C}$  ( $\pm 120$   $^{\circ}\text{C}$ )] also records an impact event. Although this temperature is very close to those obtained on ureilites using geothermometry applied to silicates, and interpreted to record igneous processing, the observation that the graphite in this sample is completely recrystallized to nanometric grain size, indicates that it records a shock event.

# 1 INTRODUCTION

The main aim of this bachelor thesis is to investigate the graphite from the ureilite sample Yamato 74123 by micro-Raman Spectroscopy to obtain the temperature recorded by this carbon phase in order to constrain its thermal history.

Scanning Electron Microscopy and micro-Raman Spectroscopy were carried out at CEASC (Centro di Analisi per la Certificazione) of University of Padua and at the Earth and Environmental Science Department of University of Pavia respectively. The project was performed in collaboration with the Natural History Museum Vienna and with Cyrena A. Goodrich of Lunar and Planetary Institute in Houston.

## 1.1 Ureilites

Ureilites represent the second largest group of achondrites and their evolutionary history is still under discussion among the scientific community. In particular, in the last years there is a huge debate about the origin of carbon phases contained in these meteorites.

As reported by Goodrich et al. 1992, ureilites appear to be highly fractionated igneous rocks either magmatic cumulates (Berkley et al., 1976; 1980; Goodrich et al., 1987a) or partial melt residues (Boynton et al., 1976; Scott et al., 1992) and thus the products of planetary differentiation processes. These assumptions were made considering the mineralogy, the textures and fabrics, the lithophile element chemistry, and some aspects of Sm-Nd isotopic systematics (Berkley et al. 1976) observed in these meteorites (Goodrich et al. 1992). Ureilites mainly differ from the other stony meteorites and in comparison with chondrites they are enriched in Mg but depleted in metal, troilite, alkaline elements. They contain large olivine grains and few smaller low Ca clinopyroxene (pigeonite) aggregates. Minor phases are kamacite (Ni content being 1.5-4 %), troilite FeS (1-2%), chromite (1-2%)

and carbon material (8.5%). Carbon material is represented by diamond (usually with stacking disorder), graphite and organic material.

Ureilites present different shock levels, which are very important for constraining the evolutionary history experienced by these meteorites. Shock level determination in meteorites was proposed by Stöffler et al. (1991, 2018). These authors proposed six stages of shock, from S1, low shock degree to S6, high shock degree, based on shock effects in the texture of olivine and plagioclase (e.g. extinction, fractures, presence of glass or high pressure silicate phases) observed on thin sections. The shock effects in olivine have been correlated with level of shock in diamond and carbon phases in ureilites by Nakamuta et al. (2016). A typical feature of shock degree from S3 to S6 is the presence of melt veins (Rubin et al. 1997; Stöffler et al. 1991, 2018).

The process through which carbon phases formed has been debated and is still controversial among the scientific community. One of the main questions about ureilites is why they contain large amount of noble gases concentrated in carbon veins: diamond is shown to be one of the noble gas carriers, while graphite is usually gas-free. The first hypothesis about the formation of diamonds offers an answer to this question: the formation of diamonds by chemical vapour deposition (CVD). In typical chemical vapour deposition, the substrate is exposed to one or more volatility chemistry precursors which react and/or decompose on the substrate surface to produce the desired deposit. Frequently, volatile by-products are also produced. Fukunaga et al. (1987) synthesized using an experimental apparatus diamonds by CVD from gaseous mixture of H<sub>2</sub> and CH<sub>4</sub> including argon (Ar). Argon entrapped in diamond was examined by mass spectrometry to compare the results with data obtained from ureilites samples. The comparison showed many differences between Ar content in diamond and in graphite. This was consistent with the observations by Göbel et al.

(1978) who excluded graphite as a carrier of noble gases in ureilites. Few years later, a further hypothesis was proposed about the CVD formation of diamonds in ureilites stating that diamond with noble gas content was probably formed from the solar nebula (Fukunaga et al., 1987). Another interpretation about the presence of noble gases content in diamonds was proposed by Lewis et al. (1987), suggesting the primary formation of diamond by stellar condensation, based on the study of many ureilitic samples of Allende, Murchison and Indarch meteorites. The second hypothesis proposed that diamond formation in ureilites took place under static high-pressure conditions in the deep interior of a ureilite parent body (UPB) similar to the Earth's mantle diamonds. This hypothesis was proposed for the first time by Urey et al. (1956), investigating diamonds samples collected in the Canyon Diablo meteorite, which are collected in Arizona in the crater with the same name. These authors claimed that diamonds cannot be produced except under fairly high temperature and high pressure. Using thermodynamic data and the density of graphite ( $2.26 \text{ gcm}^{-3}$ ) and diamond ( $3.51 \text{ gcm}^{-3}$ ), they understood that the required minimum pressure at 1000 K and 1200 K are at 31,000 and 37,000 bars, respectively. This huge pressure can explain the formation of diamond in the deep interior of a big parent body, with dimension similar approximately to Lunar mass or greater (Urey, 1956). This hypothesis was assumed for Almahata Sitta ureilitic samples in two recent works by Miyahara et al. (2015) and Nabiei et al. (2018). Another investigation about diamonds in ureilites of Canyon Diablo showed a pronounced similar crystallographic orientation among diamond fragments (Lipschutz, 1964). These authors proposed the formation of diamond in ureilites as product of transformation of graphite after a shock event. Some experiments on meteoritic fragments of ureilites and on diamonds were carried out using X-ray diffraction and Raman spectroscopy (Nakamuta et al., 2016).

In this work we performed Scanning Electron Microscopy (SEM) and micro-Raman Spectroscopy on the fragment Yamato 74123 and the petrographic characterization on a thin

section obtained from the same fragment (NHMV-L9822), belonging to the collection of the Natural History Science Museum of Vienna.

## 1.2 Yamato meteorites

Yamato 74123 is an Antarctic meteorite that was found on 1974 by the Japanese expedition on the Yamato mountains. In Yoshida et al. (1971) the first discovery of Yamato Meteorites by an inland survey team of the Japanese Antarctic Research Expedition (JARE) in 1969 is reported. The members of the team collected three stones on the surface of the ice sheet in the south-eastern marginal area of the Yamato Mountains. They realized that these stones could have been meteorites and started to collect other possible meteorites. Back to Japan, the nine rocks collected in Antarctica were all identified as meteorites. In addition, Yoshida et al. (1971) proposed a mechanism by which meteorites concentrated in the area, involving the flow, structure, and ablation of the ice sheet (Fig.1).

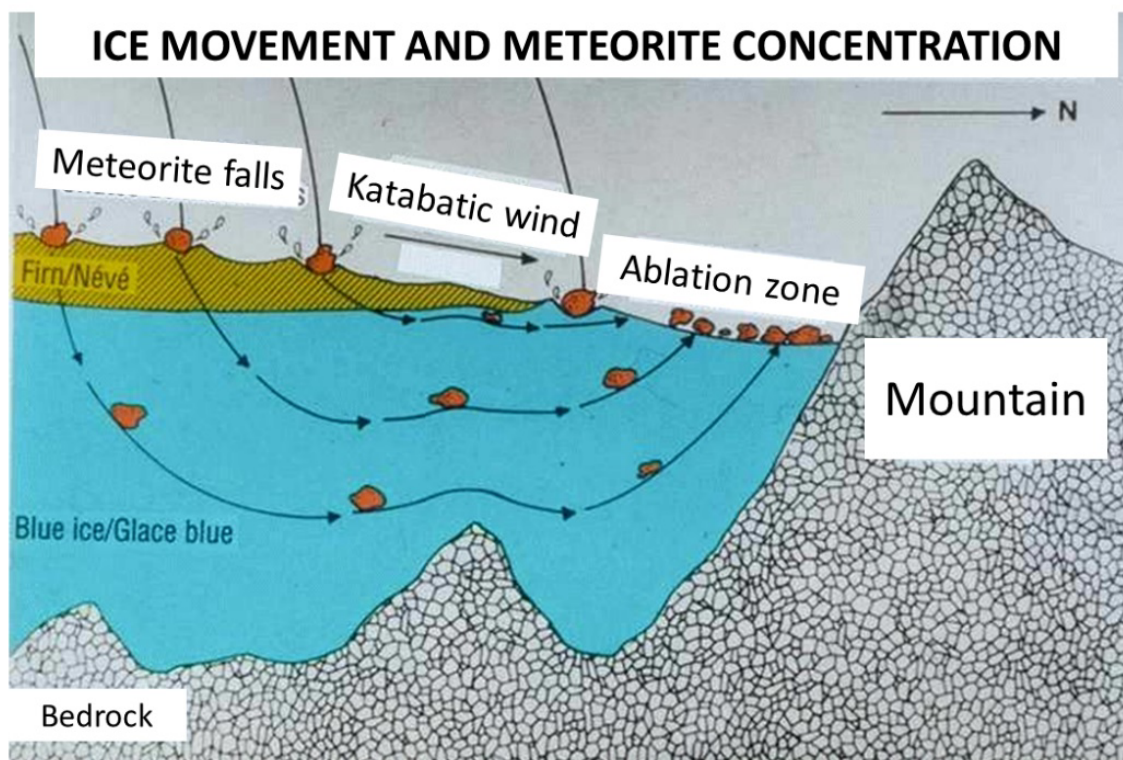


**Fig.1** In the picture ice movement and the consequently meteorite concentration is shown.



This hypothesis was developed in the field in 1969 during the collection program (Yoshida et al. 2009). After 1969 further collections of meteorites in the Yamato Mountains were conducted on 1973 and 1974, when Y-74123 ureilitic fragment was collected, and on 1975 seasons. A project involving the collection of meteorites was formally incorporated as an important component of the work undertaken by the geology group within JARE from the 1975 and 1976 seasons onwards.

## **2 SAMPLE**

### **2.1 Sample description by optical microscopy and scanning electron microscopy (SEM)**

The fragment of Yamato, Y-74123, and its thin section, NHMV-L9822, belong to the collection of the Natural History Science Museum of Vienna. Petrographic characterization of the polished thin section of Yamato 74123 was carried out at the Earth and Environmental Department of University of Pavia (Italy) by a conventional petrographic microscope in transmitted light, while the imaging and characterization of a non-carbon-coated Y-74123 ureilitic fragment was performed using low vacuum Scanning Electron Microscope (SEM), Fei Quanta 200 SEM (Fig.2) equipped with an Energy Dispersive X-ray Spectrometry (EDS) in low vacuum mode at the CEASC (Centro di Analisi e Servizi per la Certificazione) of the University of Padua (Italy). Back Scatter Electron images of Y-74123 were obtained in low vacuum mode analytical conditions, at working distance of 10.6 mm, with beam current of 93 mA and Voltage 20.00 KV with the aim to identify the graphite beds in which probably also diamonds were located.

Scanning Electron Microscopy (SEM) is a kind of electron microscopy which produces images of samples by surface scanning utilizing a focused beam of electrons. A focused electron beam (2-10 keV) scans on the surface, and several types of signals are produced and detected as a function of position on the surface. Various signals are product and they contain several information about the surface topography and composition of the sample.

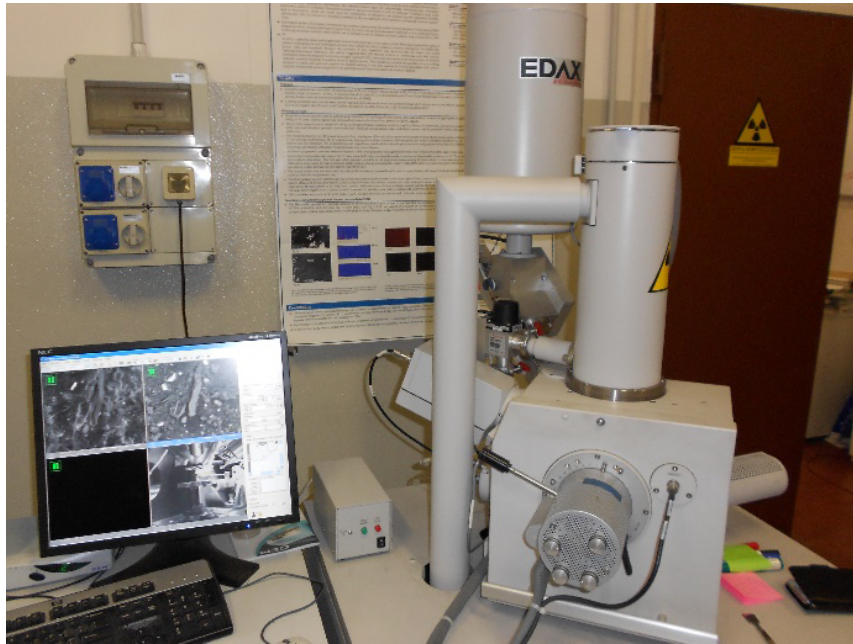


**Fig.2** Fei Quanta 200 ESEM, Scanning Electron Microscope of CEASC of University of Padua.

The investigated fragment of Y-74123 consists of aggregates of subhedral to anhedral grains, with varying amounts of interstitial pyroxenes and Si-Al-enriched glass. The sample contains coarse-grained olivine and minor clinopyroxene crystals, ranging from 0.1 to 1.5 mm, surrounded by a large amount of opaque materials (Fig.1) which are composed by carbon mixed with sulphides and metal phases. Pores and small ( $\leq 100\mu\text{m}$ ) grains of metal and sulphide are common interstitially between pyroxene grains.

The shock level of this ureilite was determined by the observation of shock microstructures in olivine in transmitted light based on the criteria proposed by Stoffler et al. (1999, 2018) and Nakamuta et al. (2016).

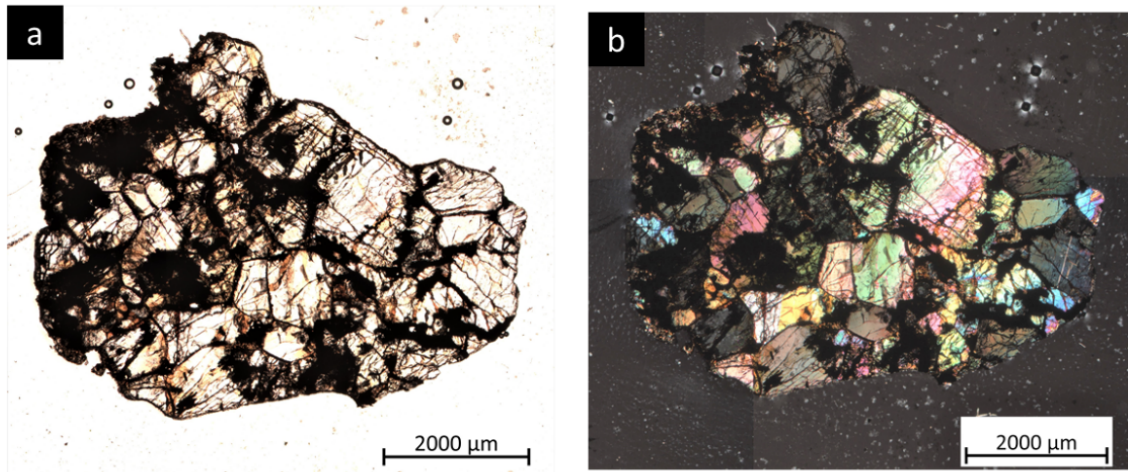


**Fig.3** Yamato 74123 thin section in parallel polarized light (a) and cross polarized light (b).

Olivine crystals show undulate extinction, planar fractures and local mosaicism. The simultaneous observation of undulate extinction and mosaicism in olivine would indicate a pressure of 15-20 GPa, corresponding to shock level S4 (Stoffler et al. 1999, 2018). In addition, both silicates (olivine and clinopyroxene) present darkening phenomena (Fig.4), caused by the dispersion of metallic Fe-Ni and sulphides within the silicate grains, which is commonly related to shock (Rubin et al. 2005). In this sample no high-pressure polymorphs of olivine, such as wadsleyite and ringwoodite, were found.

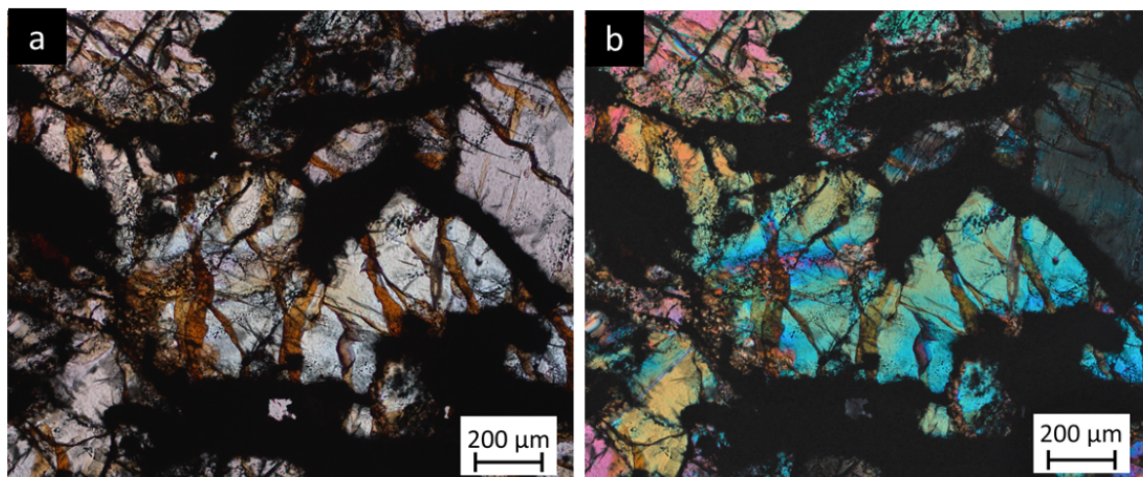


**Fig.4** Detail of olivine grains in Y-74123 in parallel polarized light (a) and in cross polarized light (b).

SEM analyses were conducted on Y-74123 with the aim to identify the graphite beds in which probably also diamonds are located. Figure 5a shows a BSE image of a carbon aggregate of the type which typically occurs interstitial to silicate phases. From carbon areas of this type we gently removed the sample that we analyzed by Raman spectroscopy. The analysis of carbon phases of the Y-74123 fragment in Figure 5b using secondary electrons and 4000x magnification clearly shows that any single aggregate is not larger than 10  $\mu\text{m}$ .

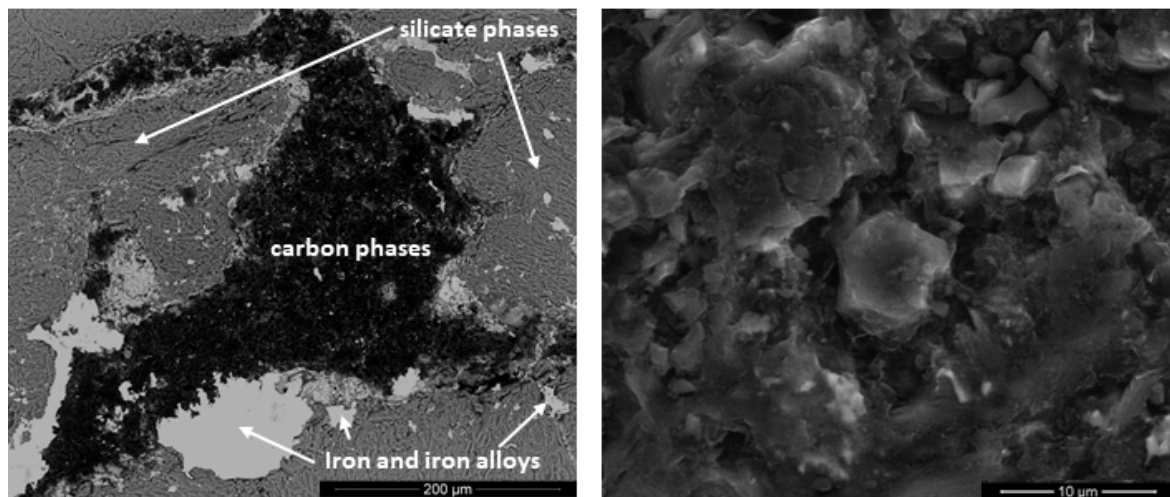


**Fig.5** (a) shows the Back scattered electron image of carbon aggregate from which we removed a carbon bearing sample and in (b) is shown a detail of figure 5a in Secondary electron In this image it is possible observe that the aggregates in the carbon phases beds are not larger than 10  $\mu\text{m}$ .

The BEI images collected by SEM were merged and analysed with ImageJ and MultiSpec software to obtain the percentage of phases observed on the surface of this fragment (Fig.6). The image analysis showed the percentage referred to the three main classes identified in the ureilitic samples: (i) silicate phases – mainly composed by olivine and pigeonite – light grey colour, (ii) carbon phases – diamond and graphite – dark grey colour and (iii) iron alloys and iron-sulphides – white colour (Figure 6a). The resulting percentages for Y-74123 are: 91% of silicate phases (olivine and pyroxene), 7% of carbon

phases and, 2% of iron alloys and iron-sulphides, respectively. The fragment was easy to be cut and polished thus suggesting a low percentage of diamonds contained on its surface. In this sample no high-pressure polymorphs of olivine, such as wadsleyite and ringwoodite, were found.

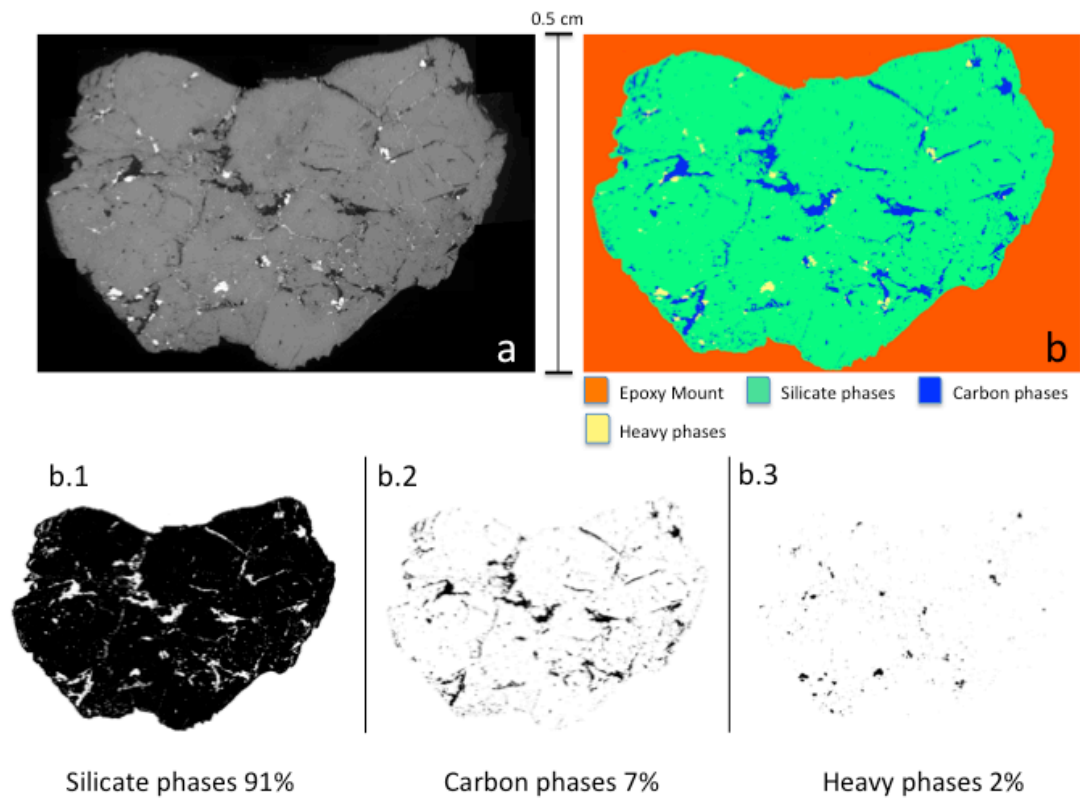


**Fig.6** (a) BSE image of Y-74123; (b) image analysis referred to (a); (b.1), (b.2) and (b.3) show the different content of silicate phases, carbon phases and iron alloy with minor troilite observed on the surface of Y-74123.

### 3 EXPERIMENTAL METHOD

#### 3.1 Micro-Raman Spectroscopy (MRS) analyses

Raman spectroscopy is a spectroscopic technique used to observe vibrational, rotational, and other low-frequency modes in a system. It depends on inelastic scattering, or Raman scattering, of monochromatic light, usually from a laser in the visible, near infrared, or near ultraviolet ranges. The laser light interacts with molecular vibrations, phonons or other excitations in the system, resulting in the energy of the laser photons being shifted up or down. The shift in energy gives information about the vibrational modes in the system.

Vibrational frequencies are characteristic of chemical bonds or groups of bonds in a specific molecule and shift of vibrational frequencies are sensitive to local environment of a molecule, such as crystal phase, local strain, and degree of crystallinity. A Raman spectrum provides a “fingerprint” representing the set of bonds present in the material (Fig. 7).

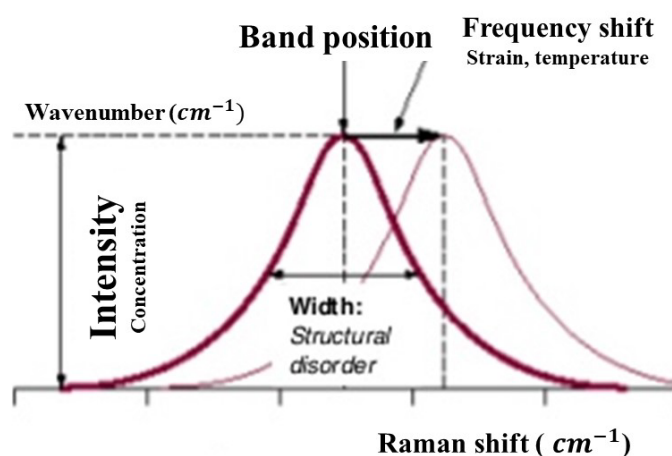


**Fig. 7** An example of Raman peak, in which the intensity, band position, frequency shift and width of the spectra are reported.

We used a geothermometric approach by Cody et al. (2008) and Ross et al. (2011) with the same procedure reported in Barbaro et al. (2020a) for the Almahata Sitta samples (AhS 209b, AhS 72, AhS A135A) to determine the crystallization temperature  $T_{max}$  recorded by graphite. MRS analysis of Y-74123 graphite was performed by high-resolution micro-Raman spectroscopy using a Horiba LabRam HR Evolution spectrometer equipped with an Olympus BX41 confocal microscope at the controlled temperature of 20(1) °C at the Department of Earth and Environmental Science of the University of Pavia. We used a 532 nm laser excitation with an operating power of 1-2 mW, a grating of 600 and a magnification of 50x, in order to avoid any graphite damage. The spectrometer was calibrated to the silicon Raman peak at 520.5  $\text{cm}^{-1}$ . The spectral resolution was than  $2\text{cm}^{-1}$  and we used a 30 seconds integration time with four accumulations for each spectrum. Curve fitting of the spectra was carried out using the software OMNIC for dispersive Raman (Thermo Fisher Scientific) adopting Gaussian + Lorentzian curves to obtain the best fit.

The temperature was estimated using equation (1), expressed in terms of Raman G-band Full Width at Half Maximum ( $\Gamma_G$ ):

$$(1) \quad T_{max}(\text{°C}) = 1594.4 - 20.4\Gamma_G - 5.8 \times 10^{-2} \Gamma_G^2$$

In Table I we reported the graphite peaks positions (G-band, D-band and D' band), the relevant  $\Gamma_G$  values for Y-74123 and the  $T_{max}$  estimated using equation (1).

In order to compare our  $\Gamma_G$  data with those published by Ross et al. (2011) and Barbaro et al. (2020a) we corrected our data for the instrumental peak broadening using a high-quality gemstone lithospheric diamond (with  $\Gamma_G = 5\text{cm}^{-1}$ ), following the same procedure as in Ross et al. (2011) (see Table II). In Table I, for each acquirement, the values of  $\Gamma_G$  used in equation (3) to obtain the  $T_{max}$  are reported: these values range between 1265 and 1334 ( $\pm 120$ ) °C.



These are slightly higher than that obtained by Ross et al. (2011) on graphite in AhS #7 ureilitic fragment ( $T_{\max}$  of  $990 \pm 120$  °C) while they agree with those obtained by Barbaro et al. (2020a) on AhS 209b, AhS 72 and AhS A135A (average  $T_{\max}$  of  $1275 \pm 120$  °C).

**Table I** Center positions for G, D and D' bands and FWHM (both in  $\text{cm}^{-1}$ ) of Y-74123. Calculated crystallization temperature,  $T_{\max}$ , is reported in the last column and was obtained using equation (3). The uncertainty on  $T_{\max}$  is  $\pm 120$  °C.

G-band center	G-band FWHM	G-band FWHM corrected	D-band center	D-band FWHM	D'-band center	D'-band FWHM	$T_{\max}$ (°C)
<b>Y-74123</b>							
1582	24	15	1356	49	1618	21	1286
1580	22	13	1354	46	1618	19	1310
1579	21	13	1349	37	1611	22	1329
1579	18	11	1356	22	1618	17	1365
1579	20	12	1351	40	1616	23	1334
1581	25	16	1350	50	1617	22	1265

## 4 DISCUSSION

MRS and the XRD analyses reported by Barbaro et al. (2020b) in Y-74123 revealed the presence of diamond and graphite aggregates in the interstitial regions of silicate grains as it is also commonly found in other ureilites (e.g. Hanneman et al., 1967, Vdovykin 1972). Moreover, diamond in this ureilitic fragment exhibits the presence of cubic and hexagonal stacked layers and nanotwins (e.g. Németh et al. 2014, Salzmann et al. 2015, Murri et al. 2019), which are considered as impact markers (e.g. Frondel and Marvin 1967, Hanneman et al. 1967). In Barbaro et al. (2020b) the XRD analysis on Yamato 74123 showed the coexistence of nano-diamonds and micro-diamonds associated with nano-graphite. In the carbon bearing aggregates we report also the presence of minor mineral phases such as metal iron and troilite. As it is also shown in Figure 6, metal iron and troilite fill the interstitial space between graphite-diamond crystals or occur at the boundaries of the graphite aggregates. These observations agree with those reported by Goodrich et al. (2020) and Nestola et al. (2020) for the Almahata Sitta and NWA 7983 samples. These two works proposed a graphite to diamond direct transformation in heterogeneous P-T fields by catalytic assistance of (Fe, Ni)-melt. It is noteworthy that the presence of metallic iron (Fe) is also evident in our sample Y-74123 (Fig. 6). As it concerns the heterogeneous PT-field, it is possible that the formation of the micrometric and nanometric size diamonds have occurred during the same impact event. The local different sizes of newly formed diamonds might be due to a heterogeneous shock distribution within heterogeneous samples. The heterogeneous distribution of shock effects is mainly ascribed to shock impedance contrast between contiguous phases and appears as local shock amplification wherever the shock impedance contrast is greater, and shock suppression wherever the impedance contrast is lower (Ogilvie et al., 2011). In this case, the presence of large, rigid, olivine crystal, separated by interstitial, relatively “soft” carbon-bearing matrix, yields a large impedance contrast between phases.

This implies that the shock pressure locally experienced by the carbon phases might have been higher than that recorded by the adjacent olivine, thus explaining the local occurrence of coarse-grained diamonds. As already proposed for the NWA 7983 by Nestola et al. (2020), also in Y-74123 the formation of  $\mu\text{m}$ -sized diamonds from graphite could be justified by the combined effect of PT-conditions together with penetration of (Fe,Ni)-melt, while the nano-diamonds could be formed by the direct transformation from graphite phase even in absence of (Fe,Ni)-melt. The occurrence of Fe and Ni compounds could explain the formation of diamond even at lower pressures compared to those estimated for diamond formed in impact cratering processes (e.g. Koeberl et al. 1997 and references therein).

The temperature recorded by graphite of this ureilite (Y-74123), close to 1100-1300°C ( $\pm 120^\circ\text{C}$ ), is similar to that reported in Barbaro et al. (2020a) and slightly higher than that reported by Ross et al. (2011) for the AhS sample. This recorded temperature could represent the temperature due to the shock event or could be the post-shock temperature, following the hypothesis made by Gillet and El Goresy (2013). We do not consider such temperature as a pre-shock temperature because it is determined on nanographite and such nanographite cannot be the pristine graphite of the UPB but a shock product.

## 5 CONCLUSIONS

New studies on carbon phases in Y-74123 provide hints on the shock history of the meteorite. The XRD analysis carried out on Y-74123 by Barbaro et al. (2020b) showed that there is the coexistence of nano-diamond together with micro-diamond and nano-graphite, in agreement with the observation by Nestola et al. (2020) for NWA 7983 sample. In addition, thanks to the MRS analyses on graphite, we obtained that (i) all samples exhibit homogeneous values of G-band centers (between 1579 and 1582  $\text{cm}^{-1}$ ) and D-band centers

(between 1349 and 1356  $\text{cm}^{-1}$ ), (ii) the  $\Gamma_G$  of graphite for the G-band ranged between 11 and 16  $\text{cm}^{-1}$ . These values provided a  $T_{\text{max}}$  close to 1200-1300  $^{\circ}\text{C}$  ( $\pm 120$   $^{\circ}\text{C}$ ).

Our results support the formation of  $\mu\text{m}$ -diamonds in Y-74123 as suggested also by Nestola et al. (2020) for the NWA 7983 sample and by Barbaro et al. (2020a, b) for the AhS and this sample. The formation occurred with the assistance of the catalytic effect of (Fe, Ni)-melt and did not require static high- pressures conditions within a large parent body. The formation of  $\mu\text{m}$  and nm-diamond and nano-graphite is more likely to be the result of an impact event or multiple events. According to Barbaro et al. (2020 a, b), the temperature recorded by graphite (close to 1200-1300 $^{\circ}\text{C}$ ) would represent the temperature related to the shock event or the post-shock temperature (Gillet and El Goresy, 2013).

In conclusion, the results from combined scanning electron microscopy and micro Raman spectroscopy studies on Y-74123 suggest that the temperature recorded by graphite could be referred to a shock event. This event could be the responsible for the diamond (both nano- and micro- diamond) formation. Moreover, a heterogeneity in the peak pressure that affected the UPB during the impact event(s) may also explain the coexistence of diamonds with different size.

## 6 REFERENCES

- Barbaro A., Domeneghetti M. C., Meneghetti M., Litti L., Fioretti A. M., Goodrich C., Christ O., Brenker F. E. Shaddad M. H., Alvaro M., and Nestola F. 2020a. Shock Temperature recorded by Graphite in Ureilites from Almahata Sitta. *51<sup>st</sup> Lunar and Planetary Science Conference (2020)*.
- Barbaro A., Domeneghetti M.C., Pittarello L., Ferrière L., Murri M., Christ O., Goodrich C. A., Alvaro M., and Nestola F. 2020b. Characterization of carbon phases of Yamato 74123 ureilite meteorite and constraints on its shock history. In prep.
- Berkley J. L., Brown IV H. G., Keil K., Carter N. L., Mercier J-C. C., and Huss G. 1976. The Kenna ureilite: an ultramafic rock with evidence for igneous, metamorphic, and shock origin. *Geochimica et Cosmochimica Acta* 40:1429-1430.
- Berkley J. L., Taylor G. J., Kiel K., Harlow G. E., and Prinz M. 1980. The nature and origin of ureilites. *Geochimica et Cosmochimica Acta* 44:1579-1597.
- Boynton W. V., Starzyk P. M., and Schmitt R. A. 1976. Chemical evidence for the genesis of the ureilites, the achondrite Chassigny and the nakhlites. *Geochimica et Cosmochimica Acta* 40:1439-1447.
- Cody G. D., Alexander C. M. O'D., Yabuta H., Kilcoyne A. L. D., Araki T., Ade H., Dera P., Fogel M., Militzer B., and Mysen B. O. 2008. Organic thermometry for chondritic parent bodies. *Earth & Planetary Science Letters* 446-455.
- Frondel C., and Marvin U. 1967. Lonsdaleite, a hexagonal Polymorph of Diamond. *Nature* 214:587-589.
- Fukunaga K., Matsuda J., Ito K., Nagao K., and Miyamoto M. 1987. Noble-gas enrichment in vapour-growth diamonds and the origin of diamonds in ureilites. *Nature* 328:141-143.
- Gillet P., and El Goresy A. 2013. Shock Events in the Solar System: The Message from Minerals in Terrestrial Planets and Asteroids. *Annual Review of Earth and Planetary Science* 41:257-285.
- Göbel R., Ott U., and Begemann F. 1978. On trapped noble gases in ureilites. *Solid Earth* 83:855-867.
- Goodrich C. A., Jones J. H., and Berkley J. L. 1987. Origin and evolution of the ureilite parent magmas: Multi-stage igneous activity on a large parent body. *Geochimica et Cosmochimica Acta* 51:2255-2273.
- Goodrich C. A. 1992. Ureilites: a critical review. *Meteoritics* 27:327-352.
- Goodrich C. A., Nestola F., Jakubek R., Erickson T., Fries M., Fioretti A. M., Ross D. K., and Brenker F. E. 2020. The Origin of Diamonds in Ureilites. *51<sup>st</sup> Lunar and Planetary Science Conference*.
- Hanneman R. E., Strong H. M., and Bundy F. P. Hexagonal Diamonds in Meteorites: Implications. *Science* 155:995-997.
- Lewis R. S., Ming T., Wacker J. F., Anders E., and Steel E. 1987. Interstellar diamonds in meteorites. *Nature* 326:160-162.
- Lipschutz M. E. 1964. Origin of Diamonds in the Ureilites. *Science* 143:1431-1434.

- Miyahara M., Ohtani E., El Goresy A., Lin Y., Feng L., Zhang J-C., Gillet P., Nagase T., Muto J., and Nishijima M. 2015. Unique large diamonds in a ureilite from Almahata Sitta 2008 TC3 asteroid. *Geochimica et Cosmochimica Acta* 163:14-26.
- Murri M., Smith R. L., McColl K., Hart M., Alvaro M., Jones A. P., Németh P., Salzmann C. G., Corà F., Domeneghetti M. C., Nestola F., Sobolev N. V., Vishnevsky S. A., Logvinova A. M., and McMillan P. 2019. *Scientific Reports* 9:10334.
- Nabiei F., Badro J., Dennenwaldt T., Oveisi E., Cantoni M., Hébert C., El Goresy A., Barrat J-A., and Gillet P. 2018. A large planetary body inferred from diamond inclusions in a ureilite meteorite. *Nature Communications* 9:1327.
- Nagata T. 1987. Magnetic properties of Antarctic meteorites, in Antarctic Meteorites. *National Institute of Polar Research* 308-337.
- Nakamuta Y., Kitajima F., and Shimada K. 2016. In situ observation, X-ray diffraction and Raman analysis of carbon minerals in ureilites: Origin and formation mechanisms of diamond in ureilites. *Journal of Mineralogical and Petrological Sciences* 4:252-269.
- Németh P., Garvie L. A. J., Aoki T., Dubrovinskaia N., Dubrovinsky L., and Buseck P. R. 2014. Lonsdaleite is faulted and twinned cubic diamond and does not exist as a discrete material. *Nature Communications* 5:5447.
- Nestola F., Goodrich C. A., Morana M., Barbaro A., Jakubek R. S., Chris O., Brenker F. E., Domeneghetti M. C., Dalconi M. C., Alvaro M., Fioretti A. M., Litasov K., Fries M. D., Leoni M., Casati N. P. M., Jenniskens P., and Shaddad M. H. 2020. Impact shock origin of diamond in ureilite meteorites. In press in PNAS journal (10.1073/pnas.1919067117).
- Ogilvie P., Gibson R. L., Reimold W. U., Deutsch A., and Hornemann U. Experimental investigation of shock metamorphic effects in a metapelitic granulite: The importance of shock impedance contrast between components. *Meteoritics & Planetary Science* 46:1565-1586.
- Ross A. J., Steele A., Fries M. D., Kater L., Downes H., Jones A. P., Smith C. L., Jenniskens P. M., Zolensky M. E., and Shaddad M. H. 2011. MicroRaman spectroscopy of diamond and graphite in Almahata Sitta and comparison with other ureilites. *Meteoritics & Planetary Science* 46 364-378.
- Rubin A. E. 1997. Mineralogy of meteorite groups. *Meteoritics & Planetary Science* 32:231-247.
- Rubin A. E. 2005. Relationships among intrinsic properties of ordinary chondrites: Oxidation state, bulk chemistry, oxygen-isotopic composition, petrologic type, and chondrule size. *Geochimica et Cosmochimica Acta* 69:4907-4918.
- Salzmann C. G., Murray B., and Shephard J. J. 2015. Extent of stacking disorder in diamond. *Diamond and Related Materials* 59:69-72.
- Scott E. R. D., Taylor G. J., and Keil K. 1992. Origin of ureilite meteorites and implications for planetary accretion. *Geophysical Research Letters* 20:415-418.
- Stöffler D., Keil K., and Scott E. R. D. 1991. Shock metamorphism of ordinary chondrites. *Geochimica et Cosmochimica Acta* 55:3845-3867.

- Stöffler D., Hamann C., and Metzler K. 2018. Shock metamorphism of planetary silicate rocks and sediments: Proposal for an updated classification system. *Meteoritics and Planetary Science* 53:5-49.
- Urey H. C. 1956. Diamonds, Meteorites, and the origin of the Solar System. *Astrophysical Journal* 124:623.
- Vdovykin G. P. 1972. Forms of Carbon in the new Haverö Ureilite of Finland. *Meteoritics* 7:547-552.
- Yoshida M., Ando H., Omoto K., Naruse R., Ageta Y. 1971. Discovery of meteorites near Yamato Mountains, East Antarctica. *Antarctic Rec.* 39:62-65.
- Yoshida M. 2009. Discovery of the Yamato Meteorites in 1969. *Polar Science* 3:272-284.

## **ACKNOWLEDGEMENTS**

Special thanks to Professor Maria Chiara Domeneghetti for her guidance and assistance during the research process. Her class in Mineralogy provided the foundation in approaching this work.

I thank Dr. Anna Barbaro for her valuable guidance for the research and for her input in the review process of this work.

I thank my family, Ennio and Simona, for their encouragement, support and motivation during my academic journey.